International Journal of Nanomedicine

Dovepress
open access to scientific and medical research

Open Access Full Text Article

ORIGINAL RESEARCH

Carrier-Free Gambogic Acid Dimer Self-Assembly Nanomedicines for Rheumatoid Arthritis Treatment

Yuling Liu[1,*], Xin Nie[2,3,*], Yihan Wu[2], Longfei Lin[1], Qian Liao[1], Jingjing Li[4], Simon Ming-Yuen Lee[3], Hui Li[1,5], Jinming Zhang[2]

[1]Institute of Chinese Materia Medica, China Academy of Chinese Medical Sciences, Beijing, People's Republic of China; [2]State Key Laboratory of Southwestern Chinese Medicine Resources, Pharmacy School, Chengdu University of Traditional Chinese Medicine, Chengdu, People's Republic of China; [3]State Key Laboratory of Quality Research in Chinese Medicine and Institute of Chinese Medical Sciences, University of Macau, Macau, Macau Special Administrative Region, People's Republic of China; [4]Department of Rehabilitation Sciences, Faculty of Health and Social Sciences, The Hong Kong Polytechnic University, Hong Kong, Hong Kong Special Administrative Region, People's Republic of China; [5]Institute of Traditional Chinese Medicine Health Industry, China Academy of Chinese Medical Sciences, Nanchang, People's Republic of China

*These authors contributed equally to this work

Correspondence: Hui Li, Institute of Chinese Materia Medica, China Academy of Chinese Medical Sciences, Beijing, People's Republic of China, Email lihuiyiren@163.com; Jinming Zhang, State Key Laboratory of Southwestern Chinese Medicine Resource, Chengdu University of Traditional Chinese Medicine, Chengdu, People's Republic of China, Email cdutcmzjm@126.com

International Journal of Nanomedicine downloaded from https://www.dovepress.com/
For personal use only.

Introduction: The insufficient targeting delivery of therapeutic agents greatly impeded the treatment outcomes of rheumatoid arthritis (RA). Despite the recognized therapeutic advantages of gambogic acid (GBA) in inflammatory diseases, its high delivery efficiency to inflammatory site still limits its clinical application. Self-assembly of drug dimers into carrier-free nanoparticles (NPs) has become a straightforward and attractive approach to develop nanomedicines for RA treatment. Herein, homodimers of GBA were designed to form the carrier-free NPs by self-assembly for RA treatment.

Methods: The synthetic gambogic acid dimers (GBA_2) were self-assembled into NPs using a one-step solvent evaporation method. The size distribution, morphology, drug-loading efficiency (DLE) and storage stability were evaluated. A molecular dynamic simulation was conducted to gain further insight into the self-assembly mechanisms of GBA_2/NPs. Besides, we investigated the cytotoxicity, apoptosis and cellular uptake profiles of GBA_2/NPs in macrophages and osteoclasts. Finally, the specific biodistribution on the ankles of adjuvant-induced arthritis (AIA) mice, and the anti-RA efficacy of the AIA rat model were assessed.

Results: GBA_2/NPs exhibited the uniform spherical structure, possessing excellent colloidal stability, high self-assembly stability, high drug loading and low hemolytic activity. Comparing with GBA, GBA_2/NPs showed higher cytotoxicity, cellular uptake and apoptosis rate against osteoclasts. In addition, GBA_2/NPs exhibited much higher accumulation in ankle joints in vivo. As expected, the systematic administration of GBA_2/NPs resulted in the greater alleviation of arthritic symptoms, cartilage protection, and inflammation, notably the reduced systemic toxicity compared to free GBA.

Conclusion: GBA_2/NPs formed GBA dimers exhibited the superior accumulation in the inflamed joint and anti-RA activity, potentially attributing to the similar extravasation through leaky vasculature and subsequent inflammatory cell-mediated sequestration ("ELVIS") effects in inflamed joint and the enhanced cellular uptake in macrophages and osteoclasts. Our findings provide substantial evidence that self-assembly of GBA_2/NPs would be a promising therapeutic alternative for RA treatment.

Keywords: gambogic acid dimers, carrier-free nanoparticles, self-assembly, rheumatoid arthritis, macrophage, osteoclast

Introduction

Rheumatoid arthritis (RA) is a chronic autoimmune inflammatory disease that can cause synovial inflammation, joint destruction, and disability, thereby severely reducing the quality of life of RA patients.[1] According to the statistics, RA affects approximately 1% of the global population and 0.28% of population in China.[2] In view of the limited

Received: 19 May 2023
Accepted: 17 September 2023
Published: 22 September 2023

© 2023 Liu et al. This work is published and licensed by Dove Medical Press Limited. The full terms of this license are available at https://www.dovepress.com/terms.php and incorporate the Creative Commons Attribution – Non Commercial (unported, v3.0) License (http://creativecommons.org/licenses/by-nc/3.0/). By accessing the work you hereby accept the Terms. Non-commercial uses of the work are permitted without any further permission from Dove Medical Press Limited, provided the work is properly attributed. For permission for commercial use of this work, please see paragraphs 4.2 and 5 of our Terms (https://www.dovepress.com/terms.php).

clinical overcomes and severe side effects of these anti-RA agents in the market, anti-inflammatory and immunosuppressive natural compounds have attracted increasing attention. Gambogic acid (GBA) is a natural compound that exhibits significant therapeutic advantages in cancer and RA treatment.[3–6] To overcome its poor aqueous solubility and undesirable biodistribution, which lead to unavoidable systemic toxicity issues,[7] a series of polymer matrix-based nano-delivery systems for GBA like micelles, nanoparticles, nanofibers, and nanorods have been developed for cancer treatment.[8,9] However, few studies have focused on targeted delivery of GBA for RA treatment. Currently, nanomedicines are thought to passively accumulate in chronically inflamed tissues via a similar extravasation through leaky vasculature and subsequent inflammatory cell-mediated sequestration ("ELVIS") effects. Previous findings have demonstrated promising opportunities for the use of nanomedicines in the RA treatment.[10–12]

However, these nanosystems based on nanocarrier materials have some common drawbacks, such as a complex drug encapsulation process, low drug loading efficiency, and poor batch-to-batch reproducibility in large-scale production.[13,14] Additionally, the repeated administration of large amounts of carrier materials in the body poses critical challenges for clinical translation owing to potential adverse side effects. Carrier-free nanomedicines generated by the self-assembly of small-molecule drugs have been proposed to effectively resolve these issues. Unfortunately, most chemotherapeutics cannot spontaneously self-assemble into nanoparticles (NPs). An approach relying on drug dimerization based on chemical linkers between small-molecule drugs has been employed to construct self-assembled nanoparticles. The strong intermolecular forces between homodimers, such as π-π stacking interactions, hydrogen bonding, and electrostatic forces, etc.[15] drive the formation of nanoassembly. Given the active chemical groups in the GBA structure, we readily synthesized the gambogic acid dimers (GBA_2) based on an ester linkage via intermolecular interactions. Simple insertion of an ester linkage can transform the GBA dimers into a uniform nanosystem in water, with three advantages: high drug loading (~85.78%, w/w), high self-assembly stability, and low hemolysis when administered intravenously.

Both macrophages and osteoclasts are key players in the persistent progression of joint inflammation and destruction. Generally, the life spans of macrophages and osteoclasts are precisely regulated by apoptosis to maintain immune homeostasis and bone function balance, respectively.[16] It was reported that targeted apoptosis of osteoclasts in arthritic joints is effective against inflammatory arthritis,[16] hence, we investigated that the cell apoptosis of GBA_2/NPs assembled by GBA dimers against osteoclasts herein. In addition, regarding the advantages of the accumulation in inflamed joints and osteoclasts, as showed in Scheme 1, the carrier-free GBA_2/NPs were designed as a novel therapeutic approach for RA treatment.

Materials and Methods

Materials

Gambogic acid (purity >98%) was purchased from Chengdu Alfa Biotechnology Co. Ltd. (China). 1-ethyl-3-(3-dimethylaminopropyl) carbodiimide hydrochloride (EDC), 4-dimethylaminopyridine (DMAP), and dichloromethane (DCM) were obtained from Shanghai Aladdin Bio-Chem Technology Co., LTD (China). Near-infrared lipophilic carbocyanine dye 1, 10-dioctadecyltetramethyl indotricarbocyanine iodide (DiR) was purchased from Mellon Biological Technology Co., Ltd. (Dalian, China). Dimethyl sulfoxide (DMSO) and Lipopolysaccharide (LPS) were purchased from Sigma-Aldrich (St. Louis, MO, USA). Fetal bovine serum (FBS), phosphate-buffered saline (PBS), Hank's balanced salt solution (HBSS), dulbecco's modified Eagle's medium (DMEM, Gibco), penicillin-streptomycin, and 0.25% (w/v) trypsin supplemented with 1 mM ethylene diamine tetraacetic acid (EDTA) were obtained from Invitrogen (Carlsbad, CA, USA). The cell counting kit-8 (CCK-8) assay kit and Annexin V-FITC/PI apoptosis kit were purchased from MultiSciences Lianke Biotech Co. Ltd. (Hangzhou, China). Commercial enzyme linked immunosorbent assays (ELISA) kits were obtained from Jingmei Biotech Co., Ltd. (Jiangsu, China). Anti-CD68 and Anti-CD51 antibodies were purchased from Abcam (Cambridge, UK).

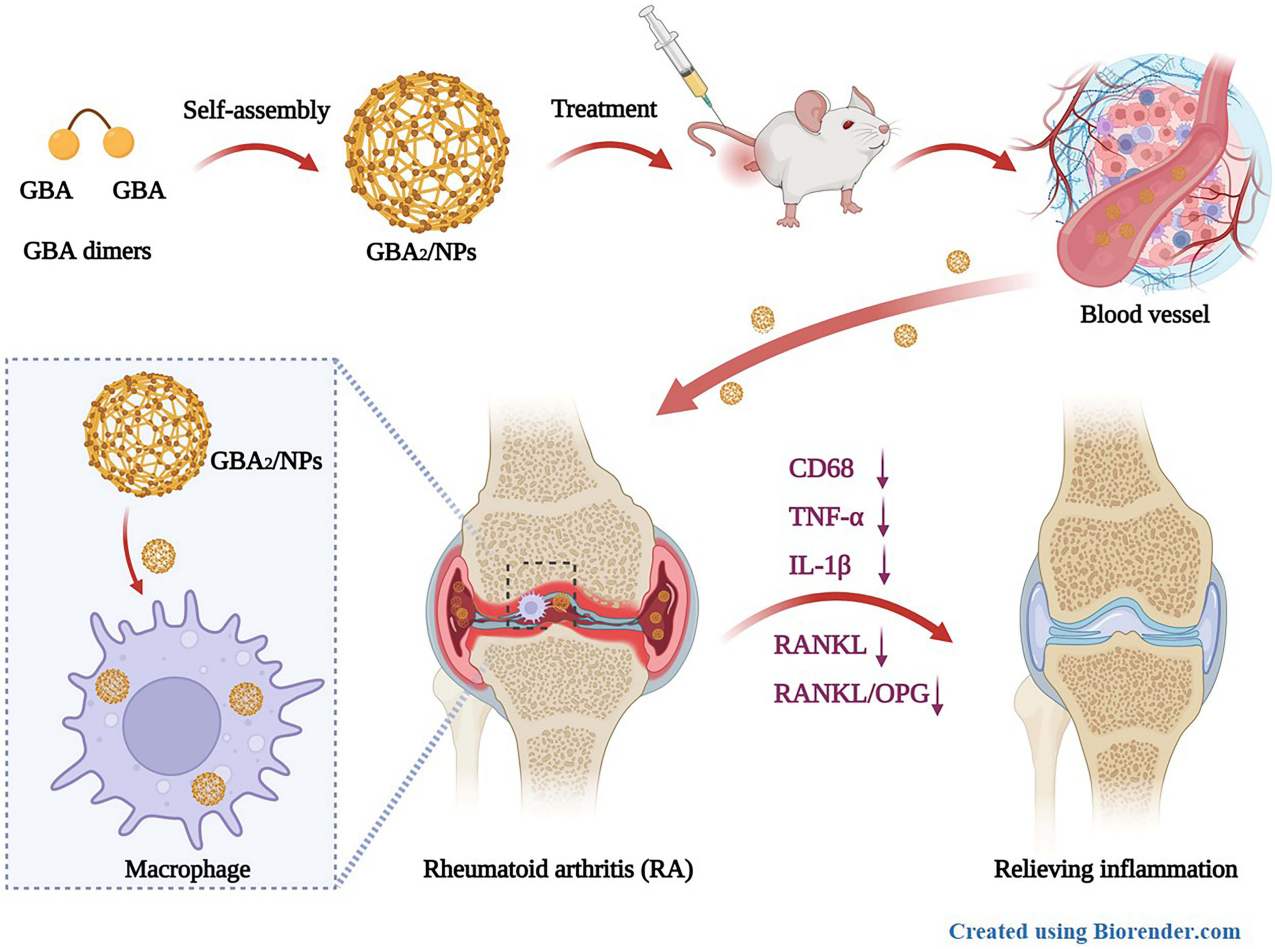

Scheme 1 Schematic representation on the therapeutic benefits GBA_2/NPs for rheumatoid arthritis treatment. (Created with BioRender.com).

The Cell Culture and Animal Studies

RAW 264.7 cells were obtained from ATCC (Manassas, VAUA) and were incubated in DMEM culture medium containing 10% FBS and 1% penicillin-streptomycin. The differentiation of RAW 264.7 cells into osteoclasts was induced by adding receptor activator of nuclear factor kappa-B ligand (RANKL) (100 ng/mL) to the α-MEM culture medium for 6 days. Cells were cultured at 37 °C in a humidified atmosphere containing 5% CO_2. Male BALB/c mice (20 ± 2 g) and male Sprague Dawley rats (200 ± 20 g) were got from SiPeiFu (SPF, Beijing) biotechnology co., LTD (Beijing, China). All animals were allowed to acclimate for one week before the experiments and were provided with a fresh diet as well as free access to water. Ethic approval for animal experiments was obtained from the Chengdu University of Traditional Chinese Medicine (CDUTCM, permit CDU2022S156). Animal experiments were complied in accordance with the national standards of the People's Republic of China (Laboratory animal: Guideline for ethical review of animal welfare [GB/T 35892–2018], Guideline of assessment for humane endpoints in animal experiment [RB/T 173–2018]). Animal welfare was ensured during whole animal experiments.

The Synthesis of Gambogic Acid Dimers

Gambogic acid dimers were synthesized by coupling two GBA molecules with EDC and DMAP as the catalysts (Figure 1A). GBA (1.0 eq), EDC (1.5 eq), and DMAP (1.5 eq) were dissolved in DCM. The reaction was performed in the dark at room temperature for 24 h, and the solvent was evaporated under reduced pressure on a rotary evaporator. The reaction mixture was purified using silica gel column chromatography to afford GBA_2 as a yellow solid. ^{1}H nuclear magnetic resonance (^{1}H NMR), ^{13}C nuclear magnetic resonance (^{13}C NMR) and MALDI-TOF/TOF-MS profiles

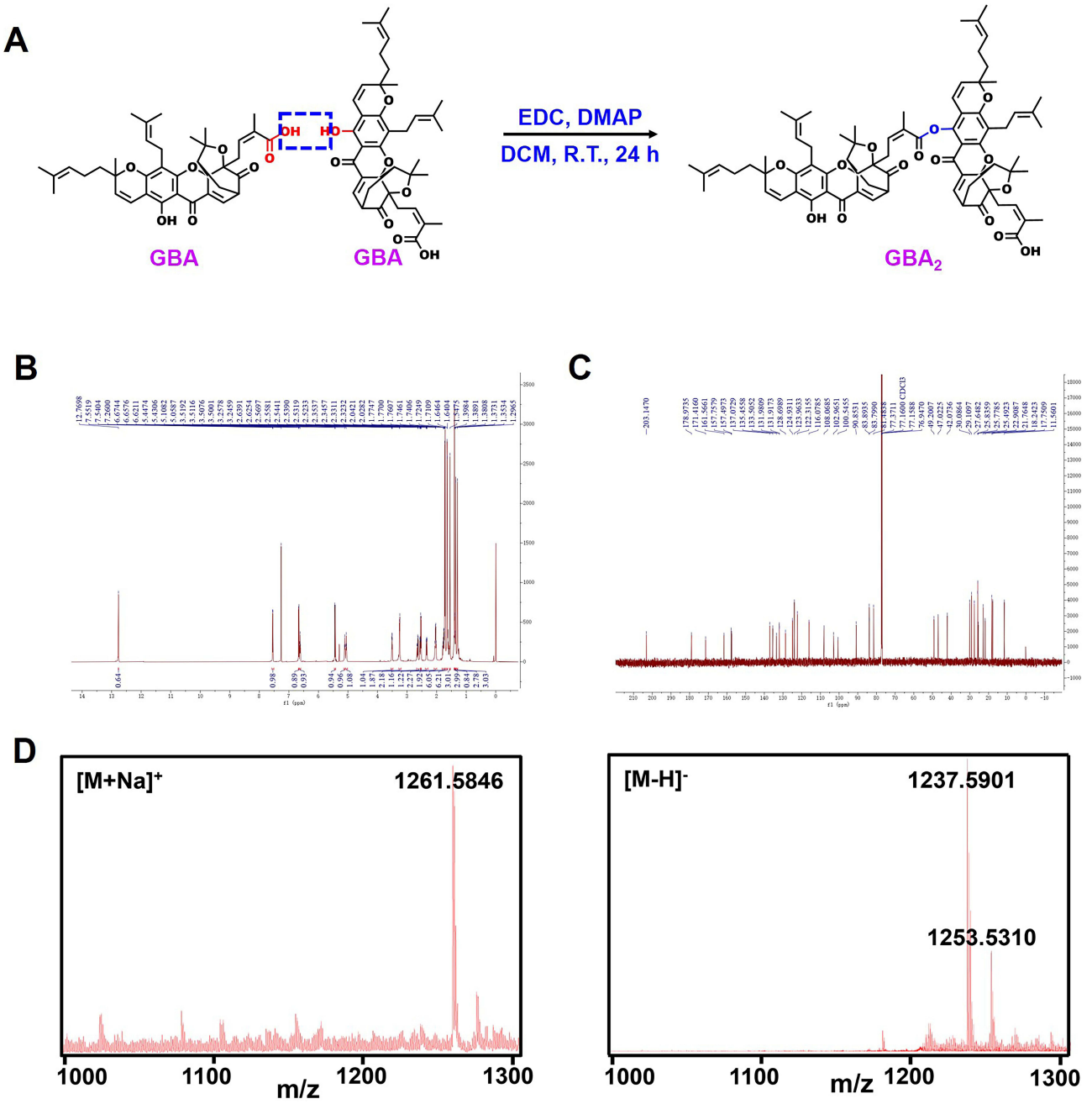

Figure 1 Identification of GBA_2. (**A**) Synthesis route of GBA_2. (**B**) ^{1}H NMR spectrum of GBA_2. (**C**) ^{13}C NMR spectrum of GBA_2. (**D**) MALDI-TOF/TOF-MS profile of GBA_2 showing the expected molecular weight.

confirmed the chemical structure of dimers. ^{1}H NMR and ^{13}C NMR spectra of GBA_2 in $CDCl_3$-d_6 solution were recorded on a Bruker Ascend 600 spectrometer with ^{1}H resonance frequency of 600 MHz and ^{13}C resonance frequency of 150 MHz, respectively. For MALDI-TOF-MS analysis, 1 μL of the sample was placed on MALDI target plates and immediately mixed with 1 μL 2, 5-dihydroxybenzoic acid in 50% acetonitrile/0.1% trifluoroacetic acid (TFA). Laser-desorbed positive and negative ions were analyzed after acceleration at 29 kV in linear mode on a Bruker ultrafleXtreme instrument (Bruker Daltonik, Bremen, Germany).

Preparation of Gambogic Acid Dimer Nanoparticles

Gambogic acid dimers were dissolved in a small amount of organic solvent and then added dropwise into deionized water under vigorous stirring to self-assemble the GBA_2/NPs using a one-step solvent evaporation method without using any surfactants or adjuvants. Briefly, 4 mg of GBA_2 was dissolved in 1 mL) acetone, which was then dropped into 10 mL of deionized water at 50 °C under continuous stirring. GBA_2 was successfully self-assembled within 2 h. The organic solvent was evaporated. Finally, the unloaded GBA_2 was removed a 0.45 μm filter (Millipore, USA). The obtained GBA_2 /NPs were stored at 4°C.

Characterization of Gambogic Acid Dimer Nanoparticles

The size distribution, polydispersity index (PDI), and ζ-potential of GBA_2/NPs were determined by dynamic light scattering (DLS) using a LITESIZER 500 laser particle analyzer (Anton Paar, Austria). The morphology of the GBA_2 /NPs was observed using transmission electron microscopy (TEM, Hitachi-7800, Japan) and scanning electron microscopy (SEM, Zeiss Sigma 300, Germany). The drug-loading efficiency (DLE) of the GBA_2/NPs was determined by high performance liquid chromatography (HPLC) using a standard curve method. Briefly, 1 mL GBA_2/NPs were mixed with methanol (1 mL). The mixture was then ultrasonicated for 30 min to extract GBA_2. After filtration through 0.22 μm filters, 10 μL of the suspension was injected into the HPLC system. The amount of GBA_2 was measured with a C18 reversed phase column (250 mm ×4.6 mm, 5 μm) at 30 °C at the maximum absorption wavelength of 360 nm. The mobile phase was a methanol–0.1% phosphoric acid–water solution (Table 1, v/v), and the flow rate was 1.0 mL/min.

$$\text{DLE (wt\%)} = \text{free drug weight in nanoparticles/weight of feeding drug} \times 100$$

The storage stability of GBA_2/NPs at 4°C was evaluated by measuring the particle size and PDI using DLS during the storage period. Additionally, a serum stability test was performed. GBA_2/NPs were mixed with FBS at 1:1 (v/v) ratio, which was gently shaken at 37 °C. The supernatant of the mixture was collected at specific time points (0, 0.5, 1.0, 1.5, 2.0, 2.5, 3.0, 3.5, and 4.0 h), and the absorbance at 560 nm was measured using a microplate reader (SpectraMax iD5, USA).

In vitro hemolytic activity of GBA_2/NPs was evaluated. A 2% red blood cells (RBCs) suspension was obtained from rabbit heart blood as described in previous study.[17] About 0.5 mL of the RBC suspension was incubated with 0.5 mL of free drug and nanoparticles at equivalent GBA concentrations (1.0, and 2.0 μg/mL) at 37 °C. After 4 h, the samples were centrifuged at 3000 rpm for 10 min. Absorbance (A) of the supernatant was measured using a microplate reader at 545 nm. RBC suspensions incubated with normal saline and distilled water were used as negative (0% lysis) and positive controls (100% lysis), respectively. The hemolytic rates of the samples were calculated using the following formula:

$$\text{Hemolytic rate}(\%) = \frac{A_s - A_n}{A_p - A_n} \times 100\%$$

Where A_s represents the absorbance value of the samples and A_n and A_p are the negative and positive controls, respectively.

Table 1 Information of Mobile Phase System

t/min	Methanol	0.1% Phosphoric Acid Water Solution
0–10	85	15
10–30	88	12
30–40	90	10
40–50	90	10

Molecular Dynamics Simulation

To gain further insight into the self-assembly mechanisms, the molecular dynamics simulations were conducted. CHARMM-GUI was used to construct the GBA_2 molecules. All MD simulations were performed using GROMACS software. The results are presented in VMD-1.9.2. The model system was composed of 25 GBA_2 molecules and 7000 water molecules. The side length of the water box was initially set to 10 nm. First, energy minimization was performed, and then a 1 ns simulation in the NPT ensemble. Finally, the size of the simulation box was 7*7*7 nm^3, followed by a 100 ns balance simulation (NPT,298 K, 1atm).

Biological Evaluation in vitro

The viability of GBA and GBA_2/NPs on Raw 264.7 cells was evaluated using the cell count kit-8 (CCK-8). RAW 264.7 cells were seeded in 96-well plates (8×10^3 cells/well) for 24 h in advance. The cells were then cultured in 0.5% FBS medium containing free GBA and GBA_2/NPs at equivalent GBA concentrations (0–8 μM) for another 24 h. Based on kit instructions, 10 μL CCK-8 solution was added to measure the absorbance at 450 nm with a microplate reader (SpectraMax iD5, USA) to evaluate cell viability. Besides, we investigated the cellular uptake to observe the difference between GBA_2/NPs and free drug. RAW 264.7 cells were seeded at a density of 2.5×10^5 cells/well in 6-well plates and incubated for 24 h to allow cell attachment. Following that, cells were treated with free GBA or GBA_2/NPs at equivalent GBA concentrations (100 μg/mL) for 4 h at 37°C. The cells were then washed thrice with cold Hank's balanced salt solution (HBSS). Next, the cells were collected, freeze-thawed thrice, and ultrasonicated for 15 min. The lysate was extracted with methanol (0.5 mL), mixed by vibration, and centrifuged at 15,000 rpm for 5 min. Ten microliters of the resulting supernatant were used for the measurement of GBA_2 in the samples by HPLC analysis. Analytical conditions for gambogic acid dimers followed what we described above, while that of GBA was as follows: mobile phase, methanol −0.1% acetic acid water solution (93:7, v/v); detection wavelength, 360 nm; column, C18; column temperature, 25 °C; flow rate: 1.0 mL/min. In this study, the cytotoxicity and cellular uptake of GBA and GBA_2/NPs were also evaluated in osteoclasts. The inadequate apoptosis of osteoclasts in the RA joint contributes toward the persistent progression of joint inflammation and destruction.[16] To investigate whether GBA_2/NPs could effectively induce the apoptosis of osteoclasts, the apoptotic profile was determined by flow cytometry assay.

Biodistribution of Gambogic Acid Dimer Nanoparticles in Adjuvant-Induced Arthritis Mice

To evaluate the biodistribution of GBA_2/NPs in vivo, adjuvant-induced arthritis (AIA) mice were intravenously injected with free DiR or DiR/GBA_2/NPs. BALB/c mice were injected with 50 μL Freund's complete adjuvant (FCA, 1 mg/mL) into the left-hind paw to establish the AIA model. After 17 days, AIA mice were intravenously (i.v.) injected with free DiR or DiR/GBA_2/NPs containing 1 mg/kg DiR (3 mice/group). At selected time points post-injection (2, 4, 6, 8, 24, 30, and 48 h), the mice were anesthetized with isoflurane and observed using an in vivo imaging system (IVIS) (PerkinElmer, USA). At the end of the experiment, the mice were euthanized. The heart, liver, spleen, lungs, kidneys, and hind limbs were harvested for the ex vivo imaging of DiR fluorescence.

Anti-Rheumatoid Arthritis Efficacy of Gambogic Acid Dimer Nanoparticles in Adjuvant-Induced Arthritis Rats

The anti-RA effects of GBA_2/NPs were evaluated in AIA rats that were intracutaneously injected with 50 μL of FCA (10 mg/mL) into the left-hind footpads. After 17 days, the rats were randomly divided into three groups (n = 8), which were intravenously injected with saline, free GBA (4 mg/kg), or GBA_2/NPs (equivalent GBA dosage of 4 mg/kg) twice weekly. Healthy rats were treated with saline as a control group. The body weight, left-hind paw volume, and paw thickness were measured twice per week. Survival was monitored throughout the experimental period. On the 31st day, the rats were sacrificed and whole blood, major organs, and ankle joints from each group were collected. First, the ankle joints were fixed in 4% paraformaldehyde and scanned using ex vivo micro-computed tomography (micro-CT, PerkinElmer, 230 Inc. USA). The dataset was then reconstructed to obtain 3D images. Bone mineral density (BMD),

trabecular number (Tb.N), trabecular bone thickness (Tb.Th), and trabecular separation (Tb.Sp) were quantitatively analyzed. Subsequently, the ankle joints were immersed in 15% tetrasodium ethylenediaminetetraacetic acid (EDTA) solution for 2 months for decalcification. The decalcified joints were embedded in paraffin and sectioned for H&E, safranin O, toluidine blue, tartrate-resistant acid phosphatase (TRAP), CD68, RANKL, TNF-α, and IL-1β staining. Additionally, the joints were sectioned for TUNEL, anti-CD68, and anti-CD51 costaining. Second, whole blood was prepared to determine red and white blood cell counts using an automated hematology analyzer (Tecom, China). Serum was extracted from the whole blood. Serum levels of TNF-α, IL-1β, RANKL, osteoprotegerin (OPG), total alanine aminotransferase (ALT), aspartate aminotransferase (AST), blood urea nitrogen (BUN), and creatinine (CRE) were measured using commercial ELISA kits. Finally, the main organs (heart, liver, spleen, lung, and kidney) were collected, fixed in 4% paraformaldehyde solution, embedded in paraffin, and stained with H&E and TUNEL.

Statistical Analysis

GraphPad Prism 8.0.1 (GraphPad Software, San Diego, USA) was employed for statistical analysis. All data were expressed as mean ± standard error of mean. One-way ANOVA with Tukey's post-hoc test was performed for multi-group comparisons, and *P < 0.05 was considered statistically significant.

Results and Discussion

Identification of Gambogic Acid Dimers

Gambogic acid dimers were synthesized via esterification. ^{1}H NMR (Figure 1B), ^{13}C NMR (Figure 1C), and MALDI-TOF/TOF-MS profiles (Figure 1D) indicated successful dimerization. Yield 58.8%. ^{1}H NMR (600MHz, $CDCl_3$-d_6): δ 12.77 (s, 1H), 7.55 (d, J = 6.9 Hz, 1H×2), 6.67 (d, J = 10.1 Hz, 1H×2), 6.64–6.60 (m, 1H×2), 5.44 (d, J = 10.1 Hz, 1H×2), 5.11 (t, J = 6.9 Hz, 1H×2), 5.06 (t, J = 6.9 Hz, 1H×2), 3.51 (dd, J = 7.0, 4.5 Hz, 1H×2), 3.25 (d, J = 7.1 Hz, 2H×2), 2.68–2.54 (m, 2H×2), 2.53 (d, J = 9.4 Hz, 1H×2), 2.34 (dd, J = 13.5, 4.8 Hz, 1H×2), 2.04 (q, J = 8.0 Hz, 2H×2), 1.82–1.74 (m, 2H×2), 1.72 (d, J = 8.4 Hz, 6H×2), 1.64 (d, J = 3.6 Hz, 6H×2), 1.55 (s, 3H×2), 1.40 (s, 3H×2), 1.38 (d, J = 5.0 Hz, 1H×2), 1.35 (s, 3H×2), 1.30 (s, 3H×2). ^{13}C NMR (150MHz, $CDCl_3$-d_6): δ 203.15, 178.97, 171.42, 161.57, 157.76, 157.50, 137.07, 135.46, 133.51, 131.98, 131.92, 128.70, 124.93, 123.96, 122.32, 116.08, 108.07, 102.97, 100.55, 90.85, 83.89, 83.80, 81.48, 49.20, 47.02, 42.07, 30.09, 29.11, 27.65, 25.84, 25.78, 25.49, 22.91, 21.76, 18.24, 17.75, 11.56. MALDI-TOF/TOF-MS for GBA_2:1238, 1261.5846, $[M + Na]^+$; 1237.5901, $[M-H]^-$.

Characterization of Gambogic Acid Dimer Nanoparticles

According to dynamic light scattering (DLS) analysis, the hydrodynamic diameter and zeta potential of GBA_2/NPs was 178.21 ± 1.74 nm and −31.2 ± 0.3 mV, respectively (Figure 2A). It has been demonstrated that a diameter of 10 to 200 nm as well as a slightly negative charge could contribute to superior in vivo circulation time and inflamed joint targeting, known as extravasation through leaky vasculature and subsequent inflammatory cell-mediated sequestration ("ELVIS") effect.[18] The polydispersity index (PDI) was 0.13 ± 0.01, indicating a narrow size distribution. SEM and TEM were used to characterize the morphology of GBA_2/NPs. Both showed a uniformly spherical morphology with nanoscale sizes (Figure 2A). Notably, the drug loading efficiency of GBA_2/NPs was determined as 85.78 ± 3.67%. Taken together, the above results show that this carrier-free nanoplatform with a suitable size distribution, zeta potential, and ultra-high drug loading is suitable for GBA_2 delivery for RA therapy.

Subsequently, GBA_2/NPs were stored at 4 °C for one week. As shown in Figure 2B, the particle size and PDI values remained relatively constant, suggesting that GBA_2/NPs had excellent storage stability. Furthermore, no noticeable changes were observed after incubation in PBS containing 10% FBS at 37 °C for 4h (Figure 2C), indicating good serum stability of GBA_2/NPs. However, GBA is known to exhibit significant hemolytic toxicity.[19] To ensure the biosafety of GBA_2/NPs after intravenous injection, a hemolysis analysis was conducted. 2.0 μg/mL GBA exhibited obvious red blood cell membrane damage comparable to that of the positive control, whereas GBA_2/NPs at the equivalent GBA concentration showed no hemolysis (Figure 2D). As expected, the hemolytic toxicity of GBA was significantly reduced by its dimerization and self-assembly. These findings indicate its potential application in vitro/vivo studies.

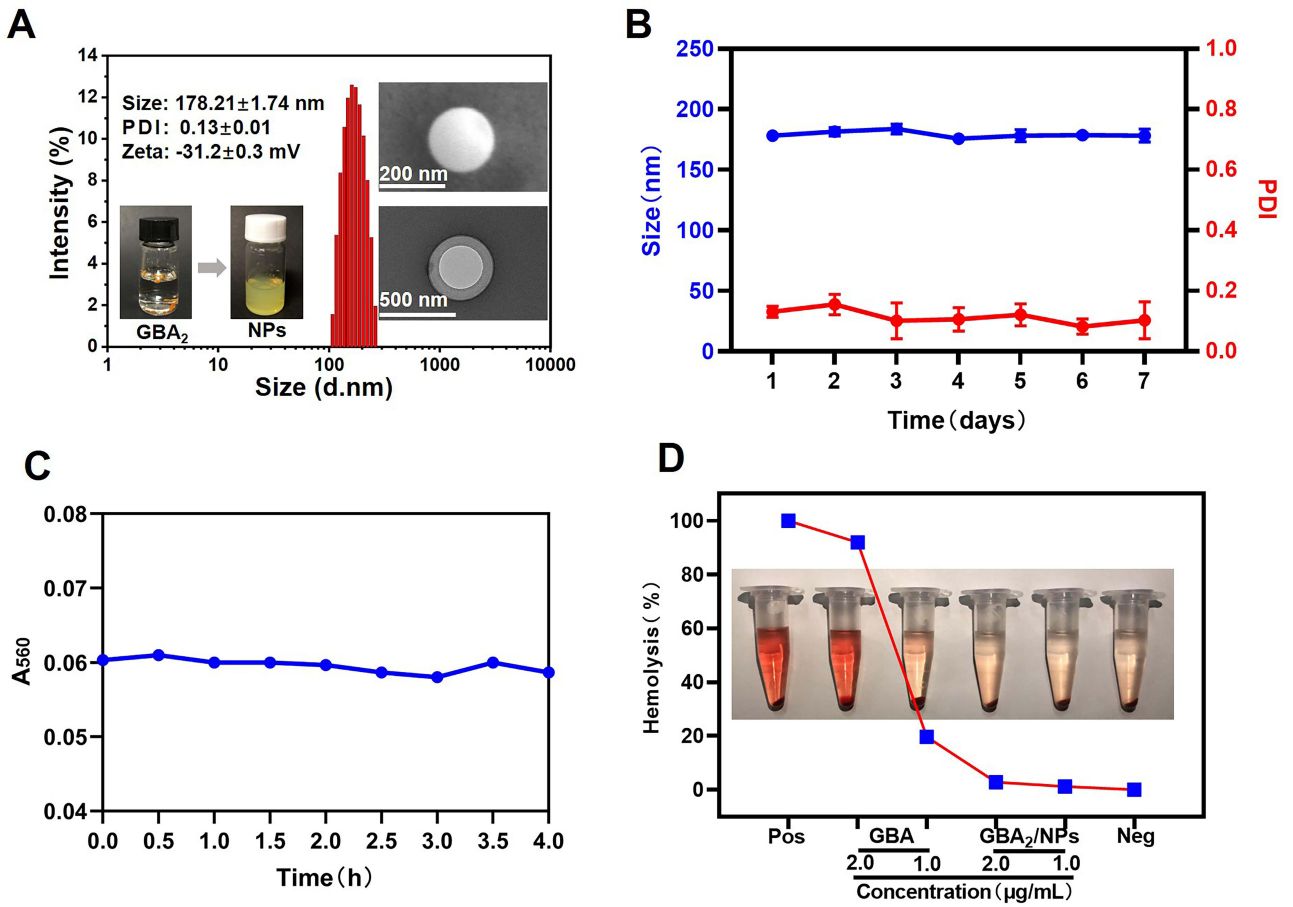

Figure 2 Characterization of GBA_2/NPs. (**A**) Particle size distribution and zeta potential by DLS, and morphology image by TEM and SEM. (**B**) Storage stability of GBA_2/NPs at 4 °C for 7 days. (**C**) The serum stability of GBA_2/NPs during 4 h incubation with 10% FBS at 37 °C. (**D**) Hemolysis assay at different concentrations of GBA or GAB_2/NPs. PBS and purified water were employed as negative and positive controls, respectively.

Molecular Dynamics Simulation of Gambogic Acid Dimer Nanoparticles

Configuration 3D diagram showed that GBA_2 self-assembled into a stable nanostructure for approximately 20 ns (Figure 3A), indicating the good self-assembly ability of the dimers. The sharp change in the solvent-accessible surface area (SASA) values also corroborated the increase in the compactness of the nanoclusters from 0 to 20 ns, which can reduce the surface area of the dimers exposed to water (Figure 3B). Analysis of the molecular interaction patterns further illustrated that hydrogen bonds (red dotted line) were the main driving force, as shown in (Figure 3C). Further calculations over a simulation time of 100 ns revealed that the number of GBA_2−water hydrogen bonds decreased, particularly from 0 ns to 20 ns, probably because of the increased aggregation of GBA_2 which kept the hydrogen bond acceptor and donor of GBA_2−water away and prevented hydrogen bond interactions (Figure 3D). According to thermodynamic laws, negative values of the free binding energy indicate favorable stability of the system.[20] As shown in Figure 3E, the absolute value of the potential energy between GBA_2 and water at 20 ns is smaller than that at 0 ns, indicating an unstable structure between them. GBA_2 preferentially forms intramolecular hydrogen bonds with water molecules. These findings demonstrate that the amphiphilic properties of GBA_2 contribute to the self-assembly process via hydrogen bonding and hydrophobic interactions.

Biological Evaluation of Gambogic Acid Dimer Nanoparticles in vitro

Cytotoxicity of GBA_2/NPs on Raw 264.7 cells was assessed after 24 hours incubation. The IC_{50} values of GBA and GBA_2/NPs were 1.476 μM and 2.531 μM, respectively. Compared to GBA, GBA_2/NPs showed lower dose-dependent cytotoxicity, which might be attributed to the enhanced cell uptake efficiency of the dimeric GBA nanoassemblies

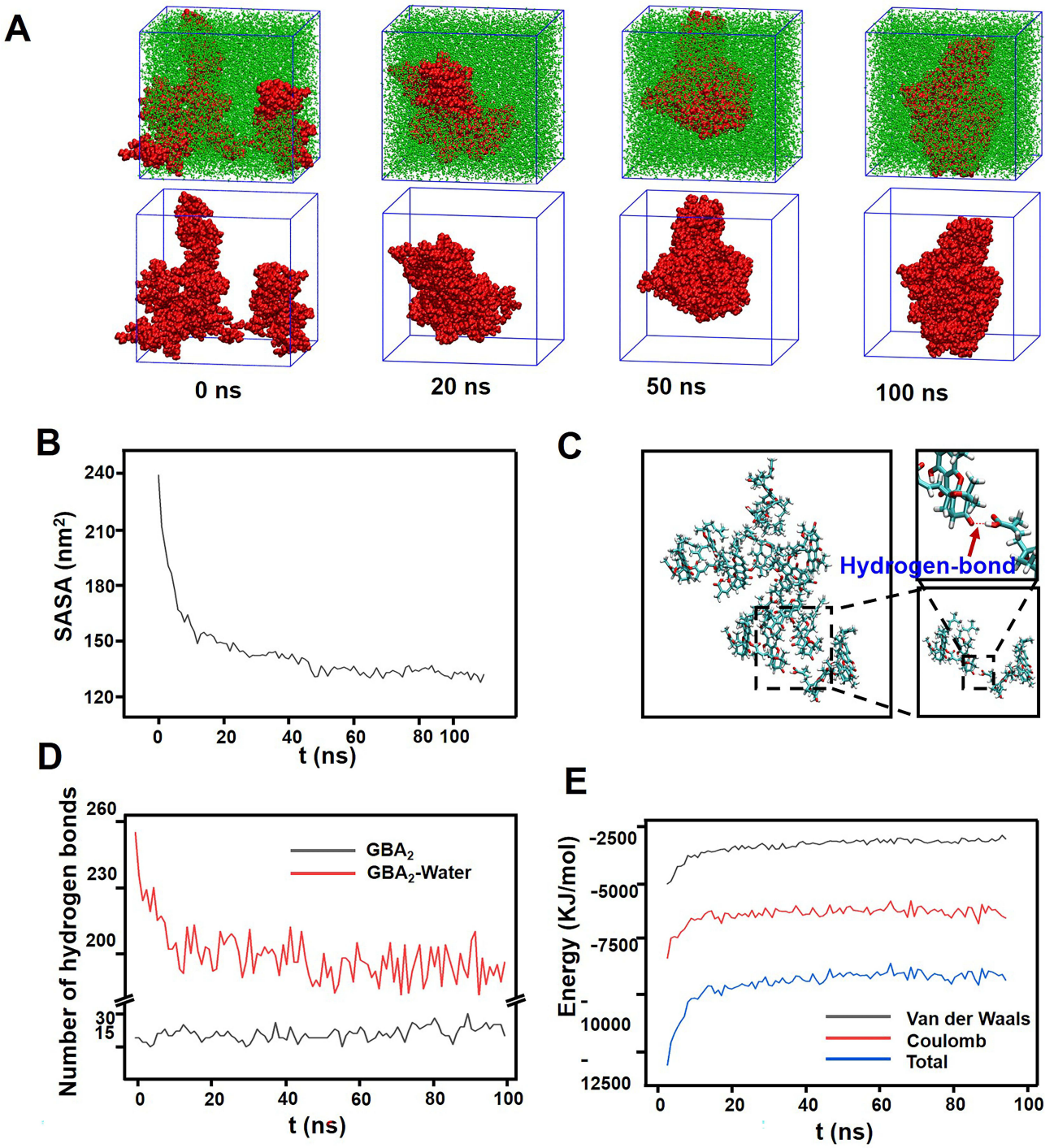

Figure 3 Molecular dynamics simulation of GBA_2/NPs. (**A**) Instantaneous simulation snapshots of the equilibrated system (GBA_2 dispersed in water, upper panel; water was not shown for clarity, lower panel). (**B**) SASA calculation of the aggregates. (**C**) Hydrogen bond interaction of dimer nanoassemblies. (**D**) Distribution of the number of different types of hydrogen bonds during simulation time. (**E**) The binding energy between the GBA_2 and water.

(Figure 4A). High intracellular uptake efficiency is necessary for therapeutic efficacy. The in vitro cellular uptake of GBA and GBA_2/NPs at equivalent concentrations was examined on Raw 264.7 cells by HPLC. As illustrated in Figure 4B, the cellular uptake of GBA_2/NPs was approximately 2-fold higher than that of GBA, possibly because of the nanoscale size. We presumed that the targeting ability of GBA_2/NPs contributes to their biosafety. Besides, the

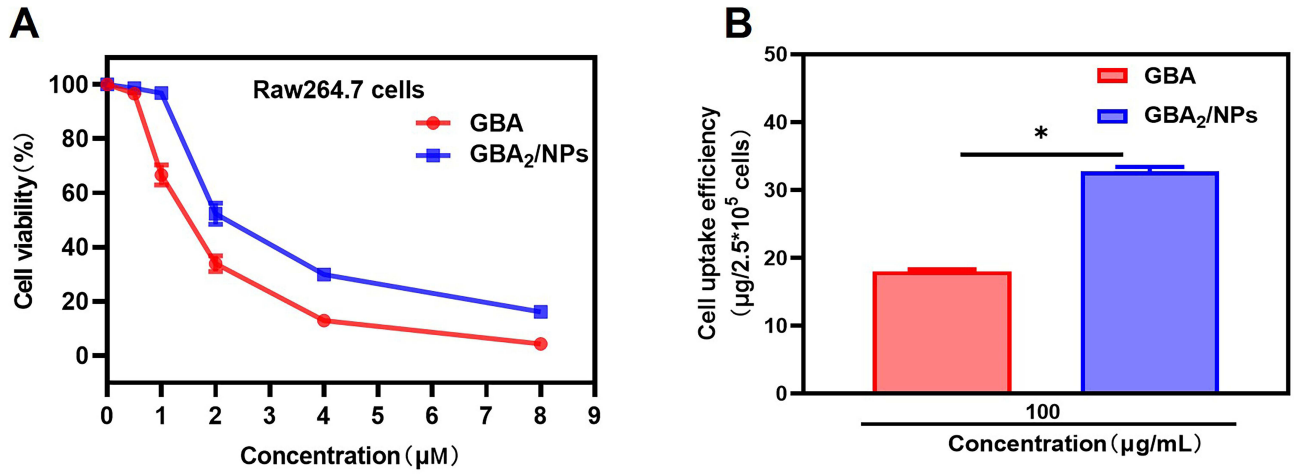

Figure 4 Cytotoxicity and cell uptake profiles of Raw264.7 cells in vitro. (**A**) Cytotoxicity of GBA_2/NPs or GBA against Raw264.7 cells with 24 h treatment. (**B**) Cell uptake of GBA or GBA_2/NPs by Raw264.7 cells at 100 μg/mL for 2 h treatment. All doses were calculated as the free GBA. *p < 0.05 indicated the significant difference.

similar results of cell viability and cellular uptake of GBA_2/NPs were shown in osteoclasts (Figures S1 and S2). Inducing the apoptosis of osteoclasts in RA joints is a promising strategy for RA therapy. In this study, the results showed that GBA_2/NPs exhibit higher apoptosis rate in osteoclasts (Figure S3), which might effectively alleviate the process of joint inflammation.

In vivo Biodistribution of Nanoparticles

The fluorescent signal in the inflamed paws of AIA mice treated with DiR/GBA_2/NPs was markedly stronger than that in the right non-inflamed paws, suggesting that DiR/GBA_2/NPs selectively accumulated in inflamed lesions. Notably, intense fluorescence was observed in inflamed paws as early as 2 h after injection of DiR/GBA_2/NPs, and the signal persisted for up to 48 h (Figures 5 and S4). In contrast, the fluorescence signal was barely detectable in the major tissues of the free DiR-treated AIA mice. Our data clearly demonstrated the rapid accumulation and prolonged circulation of GBA_2/NPs.

Therapeutic Effects of Gambogic Acid Dimer Nanoparticles in Adjuvant-Induced Arthritis Rats

Subsequently, a rat AIA model was established to investigate the therapeutic effects of GBA_2/NPs in vivo (Figure S5A). Saline, GBA, or GBA_2/NPs were intravenously injected into rats with AIA (4 mg/kg equivalent of GBA). Untreated healthy rats were used as controls. Compared with healthy rats, the thickness of the left-hind paw (Figure S5C) and volume (Figure S5B) were highest in rats treated with saline, followed by those treated with GBA or GBA_2/NPs.

Notably, GBA_2/NPs showed therapeutic effects comparable to those of GBA alone. Micro-computed tomography (micro-CT) and histological assays were used to further investigate joint destruction and synovial inflammation in different groups. Consistent with the above results, GBA and GBA_2/NPs showed similar efficacy, negligible swollen paws and ankle joints (Figure 6A), relatively smooth bone surfaces, and minor bone erosion (red arrows) (Figure 6B), together with high bone mineral density (BMD) (Figure 6F), which was close to that of healthy rats. The trabecular parameters also confirmed that GBA and GBA_2/NPs administration were equally effective in increasing the trabecular number (Tb.N) (Figure 6G) and trabecular bone thickness (Tb.Th) (Figure 6H) but decreased trabecular separation (Tb.Sp) (Figure 6I). Additionally, H&E staining revealed that both GBA and GBA_2/NPs reduced inflammatory cell infiltration (yellow arrows) and synovial hyperplasia (black arrows) (Figure 6C). Safranin-O and toluidine blue staining were used to label glycosaminoglycans, thus examining the cartilage integrity of the joint ankles.[21,22] Areas positive for safranin-O and toluidine blue staining of GBA and GBA_2/NPs were similar to those of the healthy group (Figure 6D and E), indicating that either GBA or GBA_2/NPs could recover cartilage destruction. However, our attention was drawn to the systemic toxicity of GBA, which was shown

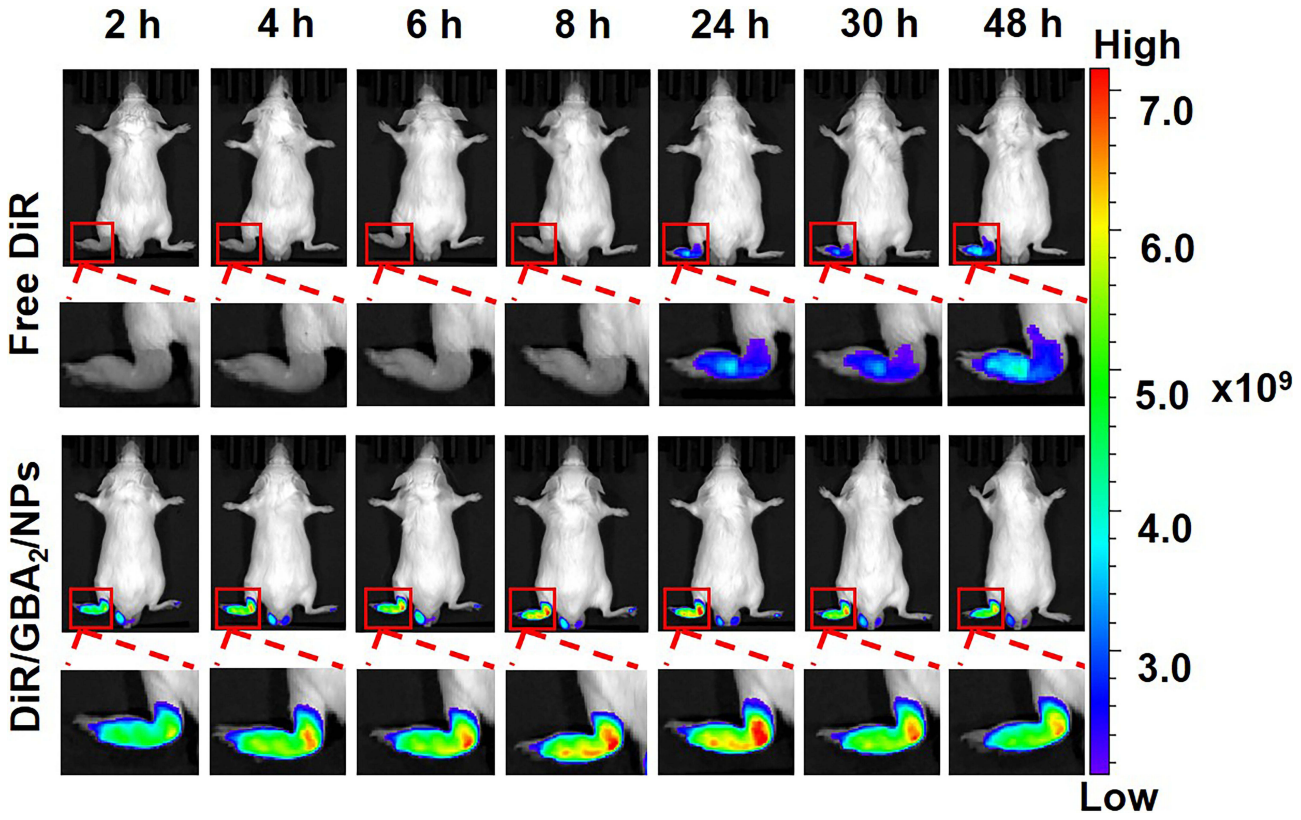

Figure 5 In vivo biodistribution of nanoparticles. Ex vivo fluorescence images showing the biodistribution of DiR and DiR/GBA_2/NPs in the mice with a unilateral inflamed joint at predetermined time intervals, ie 2, 4, 6, 8, 24, 30, and 48 h after injection.

by sharp changes in body weight (Figure S5D) and low survival rate (Figure S5E) in the rats treated with GBA. In contrast, GBA_2/NPs showed good biocompatibility. Taken together, no difference in the anti-arthritic effects between GBA and GBA_2/NPs was found, whereas the toxic effects of GBA were remarkably attenuated by the self-assembly of dimers.

Pro-Apoptotic Effects of Gambogic Acid Dimer Nanoparticles

Next, to investigate whether GBA_2/NPs could target osteoclasts and macrophages in arthritic joints and simultaneously induce apoptosis in both cell types, the level of cellular apoptosis and number of osteoclasts and macrophages in the inflamed joints were determined by TUNEL staining and immunofluorescence analysis, respectively. As shown in Figure 7A and B, GBA_2/NPs triggered a higher level of apoptosis in inflamed joints than free GBA. Furthermore, the apoptotic cells induced by GBA_2/NPs were mainly macrophages and osteoclasts, as evidenced by the overlap of green and red fluorescence. However, the GBA treatment resulted in more severe off-target apoptosis in the major organs (Figure S6). Together, these results indicate that GBA_2/NPs were preferentially enriched in inflamed joints, selectively targeted macrophages and osteoclasts, and efficiently induced apoptosis, thereby ameliorating adjuvant-induced arthritis without systemic toxicity. The reduction in osteoclasts and macrophages in inflamed lesions further confirmed the targeting activity of GBA_2/NPs. Immunohistochemical assays for CD68 expression showed that GBA_2/NPs remarkably decreased the number of macrophages (Figure 7C). Similar results can be seen in TRAP staining of osteoclasts (red area) (Figure 7D). Macrophages are the main producers of pro-inflammatory cytokines in RA, such as interleukin-1 beta (IL-1β) and tumor necrosis factor-alpha (TNF-α).[23] We observed that the GBA_2/NPs group had a lower secretion of IL-1β and TNF-α in the serum than the GBA group, which was similar to that of the healthy group (Figure 7H and I). The immunohistochemical analysis revealed that GBA_2/NPs potently decreased the expression of IL-1β and TNF-α in the ankle joint (Figure 7E and F). Furthermore, a balance between RANKL and osteoprotegerin (OPG) is essential for bone remodeling. Decreased RANKL levels and a lower RANKL/OPG ratio are helpful for RA remission.[24,25] Our study

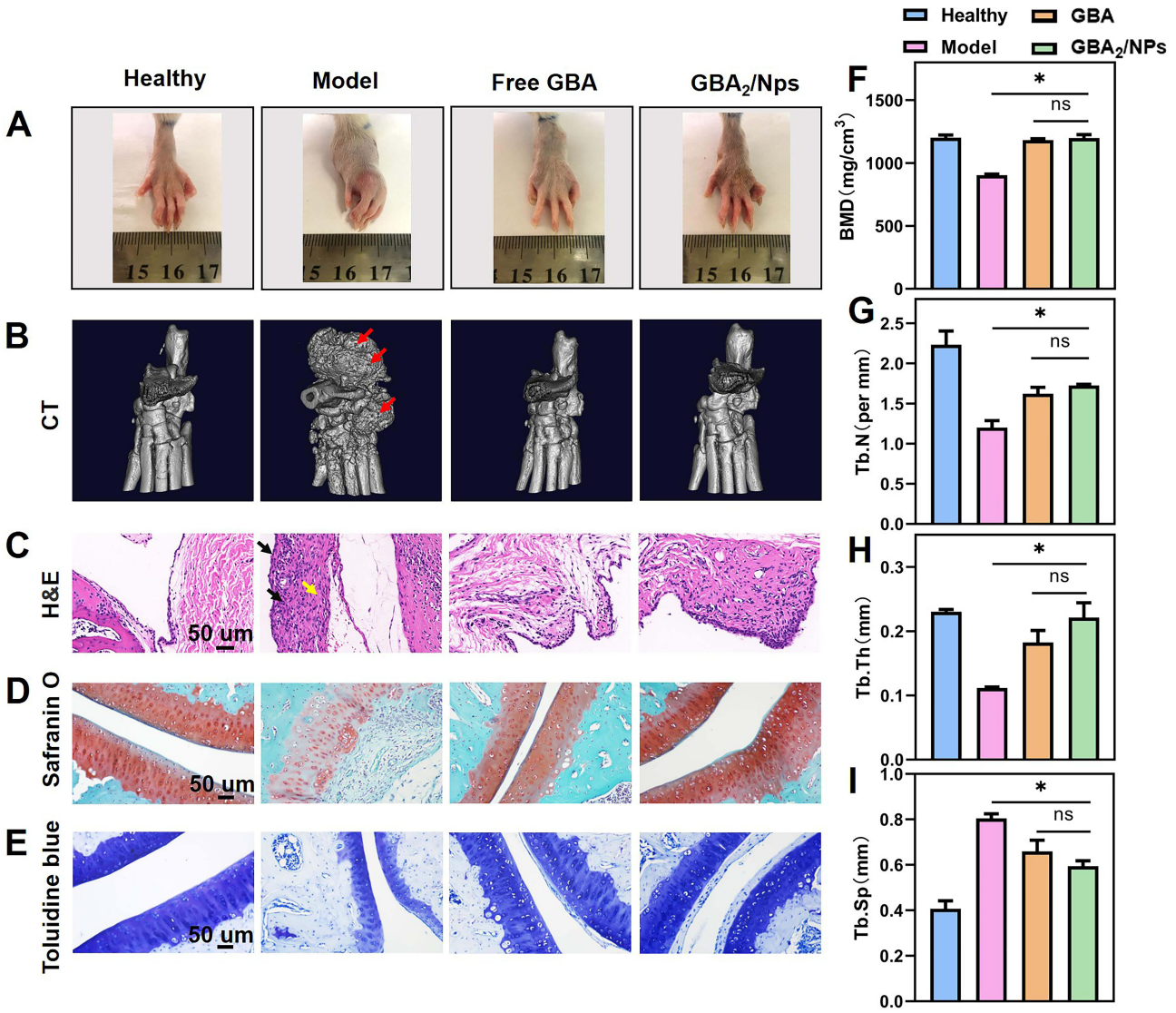

Figure 6 The administration of GBA_2/NPs influenced histopathology of AIA rats. (**A**) Representative photographs of the hindlimbs at the endpoint of the experiment from different treatment groups. Histopathology evaluation of the ankle joints was identified using (**B**) micro-CT, (**C**) H&E, (**D**) safranin-O, and (**E**) toluidine blue staining. Quantitative micro-CT analysis of (**F**) BMD, (**G**) Tb.N, (**H**) Tb.Th, and (**I**) Tb.Sp of the ankle joints. Red arrows, bone erosion; Yellow arrows, inflammatory cell infiltration; Black arrows, synovial hyperplasia. *p < 0.05 indicated the significant difference.

Abbreviations: CT, Computed tomography; H&E, Hematoxylin-eosin; BMD, Bone mineral density; Tb.N, Trabecular number; Tb.Th, Trabecular bone thickness; Tb.Sp, Trabecular separation.

found that GBA_2/NPs exhibited a recovery trend of bone function, as confirmed by the lower expression of RANKL in arthritic joints (Figure 7G), together with a smaller RANKL/OPG ratio (Figure 7J) in the serum than in the GBA group. In brief, GBA_2/NPs targeting macrophages and osteoclasts promoted apoptosis, thereby reducing inflammation and bone destruction in arthritic joints.

Considering the severe toxicity of GBA, we further evaluated the biosafety of GBA_2/NPs through histopathological analysis of major organs as well as hematological and serum biochemical examinations. As shown in Figure 8A, GBA administration resulted in histopathological abnormalities in major organs, mainly demonstrated by structural destruction (yellow arrows), necrosis (black arrows), and inflammatory cell infiltration (red arrows). ALT and aspartate aminotransferase (AST) were sensitive indicators of hepatocyte injury, whereas blood urea nitrogen (BUN) and creatinine (CRE) were those of nephrotoxicity.[26,27] The GBA group showed significant increases in BUN (Figure 8D), CRE (Figure 8E), AST (Figure 8F), and ALT (Figure 8G) levels, which indicated kidney and liver damage. White blood cells (WBC) and red blood cells (RBC) are closely associated with infection and hematological toxicity, respectively.[28] Similarly,

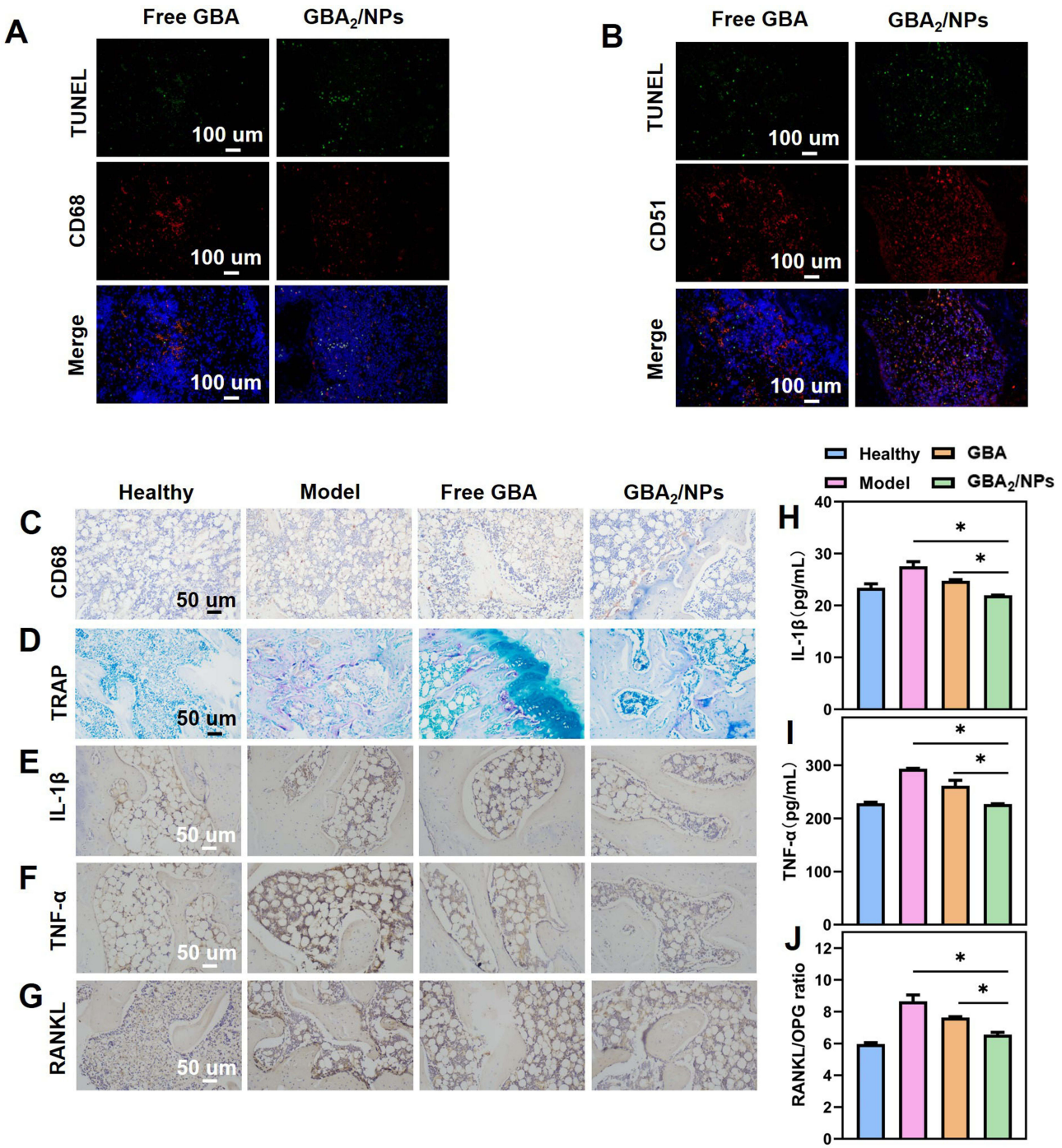

Figure 7 Pro-apoptotic effects of GBA_2/NPs in macrophages and osteoclasts in AIA rats. (**A** and **B**) Detection of apoptotic cells in ankle joints from AIA rats by TUNEL assay. Determination of macrophages and osteoclasts in ankle joints from AIA rats by immunofluorescence analysis of (**A**) CD68 and (**B**) CD51, respectively. Immunohistochemical analyses of (**C**) the CD68-stained synovial macrophages and (**D**) TRAP-stained osteoclasts in the joint tissues from rats subjected to the indicated treatment. Detection of (**E**) IL-1β, (**F**) TNF-α, and (**G**) RANKL expression levels in arthritic joints. The serum level of (**H**) IL-1β, (**I**) TNF-α, and (**J**) RANKL/OPG. *$p < 0.05$ indicated the significant difference.

Abbreviations: TRAP, Tartrate resistant acid phosphatase; IL-1β, interleukin-1 β; TNF-α, tumor necrosis factor-α; RANKL, Receptor of activator of NF-kB ligand; OPG, Osteoprotegerin.

abnormally high WBC (Figure 8B) and lower RBC counts (Figure 8C) suggest poor hemocompatibility of GBA. These adverse effects of GBA were largely abolished by the nanoassembly of GBA dimers. The structure of the cells remained intact and the nuclei were arranged in an orderly manner without necrosis or degeneration. WBC, RBC, BUN, CRE,

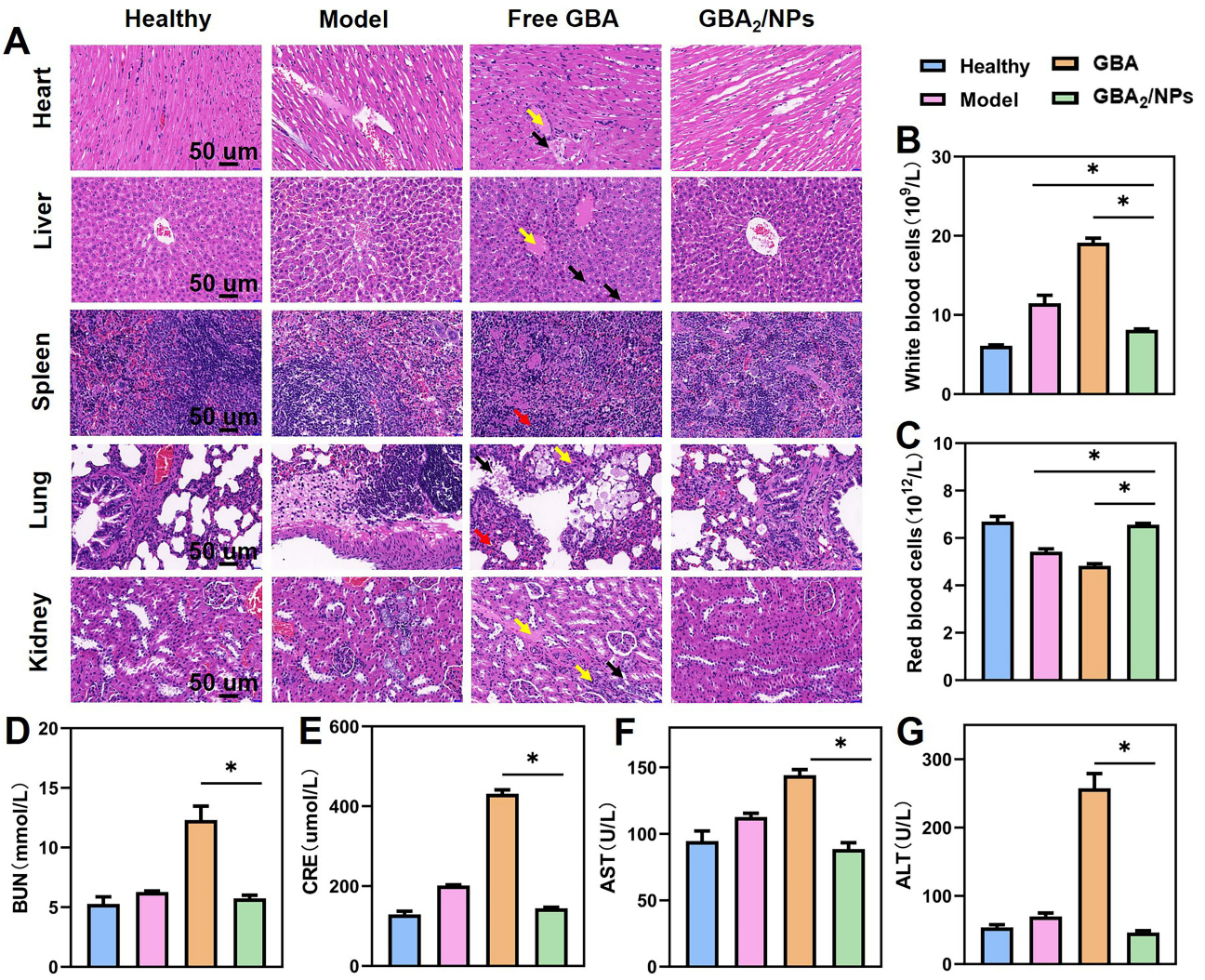

Figure 8 Reduced systemic toxicity of GBA_2/NPs in AIA rats. (**A**) H&E staining of major organs (heart, liver, spleen, lung, and kidney). The amount of (**B**) WBC, (**C**) RBC, in whole blood and the serum level of (**D**) BUN, (**E**) CRE, (**F**) AST, and (**G**) ALT in rats receiving the indicated treatment. Yellow arrows, structural destruction; Black arrows, structural necrosis; Red arrows, inflammatory cell infiltration. *p < 0.05 indicated the significant difference.

Abbreviations: WBC, White blood cells; RBC, Red blood cells; BUN, Blood urea nitrogen; CRE, Creatinine; AST, Aspartate aminotransferase; ALT, Alanine aminotransferase.

AST, and ALT levels were similar to those in the healthy rats. Collectively, these results implied that GBA_2/NPs are the safe platform for RA therapy.

Conclusion

In conclusion, GBA dimers were successfully synthesized by coupling two GBA molecules via simple insertion of an ester linkage, and conjugates could subsequently self-assemble into GBA_2/NPs driven by hydrogen bonding and hydrophobic interactions. The homodimers could self-assemble into GBA_2/NPs with extraordinarily high drug loading capacity via the facile one-step nanoprecipitation. Mediated by the "ELVIS" effect, GBA_2/NPs showed high sensitivity to inflamed joints, enabling the targeted apoptosis of macrophages and osteoclasts. The anti-arthritic efficacy of GBA_2/NPs, including inflammatory remission and bone erosion repair, was comparable to that of GBA, without systemic toxic effects. The nanoassembly of homodimers is pretty eye-catching. This study highlights the potential of nanomedicines fabricated via dimerization and self-assembly for RA therapy, which might provide new insights into the design of nano-drug delivery system with high drug loading for the treatment.

Acknowledgments

This study was supported by the Scientific and Technological Innovation Project of the China Academy of Chinese Medical Sciences (CI2021A04305, CI2021B014), Innovation Team and Talents Cultivation Program of the National Administration of Traditional Chinese Medicine (No: ZYYCXTD-D-202209), the National Natural Science Foundation of China (81803743), and Fundamental Research Funds for the Central Public Welfare Research Institutes (ZZ13-YQ -041, ZXKT21013).

Disclosure

The authors declare that they have no known competing financial interests or personal relationships that could influence the work reported in this study.

References

1. Smolen JS, Aletaha D, McInnes IB. Rheumatoid arthritis. *Lancet*. 2016;388(10055):2023–2038. doi:10.1016/S0140-6736(16)30173-8
2. Wang Q, Qin X, Fang J, et al. Nanomedicines for the treatment of rheumatoid arthritis: state of art and potential therapeutic strategies. *Acta Pharmaceutica Sinica B*. 2021;11(5):1158–1174. doi:10.1016/j.apsb.2021.03.013
3. Cascão R, Vidal B, Raquel H, et al. Potent anti-inflammatory and antiproliferative effects of gambogic acid in a rat model of antigen-induced arthritis. *Mediators Inflamm*. 2014;2014:195327. doi:10.1155/2014/195327
4. Wu X, Long L, Liu J, et al. Gambogic acid suppresses inflammation in rheumatoid arthritis rats via PI3K/Akt/mTOR signaling pathway. *Mol Med Rep*. 2017;16(5):7112–7118. doi:10.3892/mmr.2017.7459
5. Rahman M, Beg S, Verma A, et al. Phytoconstituents as pharmacotherapeutics in rheumatoid arthritis: challenges and scope of nano/submicro-medicine in its effective delivery. *J Pharm Pharmacol*. 2017;69(1):1–14. doi:10.1111/jphp.12661
6. Nguyen A, Ando H, Böttger R, et al. Utilization of click chemistry to study the effect of poly(ethylene)glycol molecular weight on the self-assembly of PEGylated gambogic acid nanoparticles for the treatment of rheumatoid arthritis. *Biomater Sci*. 2020;8(16):4626–4637. doi:10.1039/D0BM00711K
7. Hatami E, Jaggi M, Chauhan SC, et al. Gambogic acid: a shining natural compound to nanomedicine for cancer therapeutics. *Biochim Biophys Acta*. 2020;1874(1):188381. doi:10.1016/j.bbcan.2020.188381
8. Karaosmanoglu S, Zhou M, Shi B, et al. Carrier-free nanodrugs for safe and effective cancer treatment. *J Control Release*. 2021;329:805–832. doi:10.1016/j.jconrel.2020.10.014
9. Liu Y, Chen Y, Lin L, et al. Gambogic acid as a candidate for cancer therapy: a review. *Int J Nanomedicine*. 2020;15:10385–10399. doi:10.2147/IJN.S277645
10. Liu R, Luo C, Pang Z, et al. Advances of nanoparticles as drug delivery systems for disease diagnosis and treatment. *Chin Chem Letters*. 2023;34(2):107518. doi:10.1016/j.cclet.2022.05.032
11. Xin Li J, Jiao Zhang M, Feng Shi J, et al. pH-sensitive nano-polyelectrolyte complexes with arthritic macrophage-targeting delivery of triptolide. *Int J Pharm*. 2023;632:122572. doi:10.1016/j.ijpharm.2022.122572
12. Zhao J, Chen X, Ho K-H, et al. Nanotechnology for diagnosis and therapy of rheumatoid arthritis: evolution towards theranostic approaches. *Chin Chem Letters*. 2021;32(1):66–86. doi:10.1016/j.cclet.2020.11.048
13. Zhang X, Li N, Zhang S, et al. Emerging carrier-free nanosystems based on molecular self-assembly of pure drugs for cancer therapy. *Med Res Rev*. 2020;40(5):1754–1775. doi:10.1002/med.21669
14. Li S, Shan X, Wang Y, et al. Dimeric prodrug-based nanomedicines for cancer therapy. *J Control Release*. 2020;326:510–522. doi:10.1016/j.jconrel.2020.07.036
15. Fu S, Li G, Zang W, et al. Pure drug nano-assemblies: a facile carrier-free nanoplatform for efficient cancer therapy. *Acta Pharmaceutica Sinica B*. 2022;12(1):92–106. doi:10.1016/j.apsb.2021.08.012
16. Deng C, Zhang Q, He P, et al. Targeted apoptosis of macrophages and osteoclasts in arthritic joints is effective against advanced inflammatory arthritis. *Nat Commun*. 2021;12(1):2174. doi:10.1038/s41467-021-22454-z
17. Shi J, Ren Y, Ma J, et al. Novel CD44-targeting and pH/redox-dual-stimuli-responsive core-shell nanoparticles loading triptolide combats breast cancer growth and lung metastasis. *J Nanobiotechnology*. 2021;19(1):188. doi:10.1186/s12951-021-00934-0
18. Xu Y, Mu J, Xu Z, et al. Modular acid-activatable acetone-based ketal-linked nanomedicine by dexamethasone prodrugs for enhanced anti-rheumatoid arthritis with low side effects. *Nano Lett*. 2020;20(4):2558–2568. doi:10.1021/acs.nanolett.9b05340
19. Nguyen A, Rouhollahi E, Böttger R, et al. Interplay between the linker and polymer molecular weight of a self-assembling prodrug on the pharmacokinetics and therapeutic efficacy. *Biomater Sci*. 2022;10(12):3122–3136. doi:10.1039/D1BM01947C
20. Wang X, Yang B, Li L, et al. Probing the fluorination effect on the self-assembly characteristics, in vivo fate and antitumor efficacy of paclitaxel prodrug nanoassemblies. *Theranostics*. 2021;11(16):7896–7910. doi:10.7150/thno.61337
21. Wang L, Pu X, Nie X, et al. Integrated serum pharmacochemistry and network pharmacological analysis used to explore possible anti-rheumatoid arthritis mechanisms of the Shentong-Zhuyu decoction. *J Ethnopharmacol*. 2021;273:113988. doi:10.1016/j.jep.2021.113988
22. Zhang Y, Liu M, Pei R. An in situ gelling BMSC-laden collagen/silk fibroin double network hydrogel for cartilage regeneration. *Mater Adv*. 2021;2(14):4733–4742. doi:10.1039/D1MA00285F
23. Siouti E, Andreakos E. The many facets of macrophages in rheumatoid arthritis. *Biochem Pharmacol*. 2019;165:152–169. doi:10.1016/j.bcp.2019.03.029
24. Szentpétery Á, Horváth Á, Gulyás K, et al. Effects of targeted therapies on the bone in arthritides. *Autoimmun Rev*. 2017;16(3):313–320. doi:10.1016/j.autrev.2017.01.014
25. Dickerson TJ, Suzuki E, Stanecki C, et al. Rheumatoid and pyrophosphate arthritis synovial fibroblasts induce osteoclastogenesis independently of RANKL, TNF and IL-6. *J Autoimmun*. 2012;39(4):369–376. doi:10.1016/j.jaut.2012.06.001

26. Liu Y, Jin J, Xu H, et al. Construction of a pH-responsive, ultralow-dose triptolide nanomedicine for safe rheumatoid arthritis therapy. *Acta biomaterialia*. 2021;121:541–553. doi:10.1016/j.actbio.2020.11.027
27. Wang Q, Jiang H, Li Y, et al. Targeting NF-kB signaling with polymeric hybrid micelles that co-deliver siRNA and dexamethasone for arthritis therapy. *Biomaterials*. 2017;122:10–22. doi:10.1016/j.biomaterials.2017.01.008
28. Li C, Li H, Wang Q, et al. pH-sensitive polymeric micelles for targeted delivery to inflamed joints. *J Control Release*. 2017;246:133–141. doi:10.1016/j.jconrel.2016.12.027

International Journal of Nanomedicine Dovepress

Publish your work in this journal

The International Journal of Nanomedicine is an international, peer-reviewed journal focusing on the application of nanotechnology in diagnostics, therapeutics, and drug delivery systems throughout the biomedical field. This journal is indexed on PubMed Central, MedLine, CAS, SciSearch®, Current Contents®/Clinical Medicine, Journal Citation Reports/Science Edition, EMBase, Scopus and the Elsevier Bibliographic databases. The manuscript management system is completely online and includes a very quick and fair peer-review system, which is all easy to use. Visit http://www.dovepress.com/testimonials.php to read real quotes from published authors.

Submit your manuscript here: https://www.dovepress.com/international-journal-of-nanomedicine-journal